Actin Cytoskeleton Organization and Posttranscriptional Regulation of Endothelial Nitric Oxide Synthase During Cell Growth

Charles D. Searles, Lucienne Ide, Michael E. Davis, Hua Cai, Martina Weber

Abstract—Posttranscriptional regulation of endothelial nitric oxide synthase (eNOS) expression is an important mechanism by which endothelial cells respond to various physiological and pathophysiological stimuli. Previously, we showed that eNOS expression was dramatically altered by the state of cell growth and that the mechanism responsible for this regulation was entirely posttranscriptional, occurring via changes in eNOS mRNA stability. The present study identifies a role for actin cytoskeleton organization in the posttranscriptional regulation of eNOS during cell growth and examines the relationship between the state of actin polymerization and eNOS expression. We identified monomeric actin (globular [G]-actin) as the major component of a 51-kDa ribonucleoprotein that binds to the eNOS mRNA 3′ untranslated region in UV-crosslinking analysis. Binding activity of the ribonucleoprotein complex correlated with the relative concentration of G-actin versus filamentous actin (F-actin). ENOS transcripts colocalized with cytoplasmic G-actin in cells subjected to fluorescence in situ hybridization and G-actin fluorescence staining. In subcellular fractionation studies, eNOS transcripts were enriched in the free polysomal fraction of nonproliferating cells and enriched in the cell matrix-associated polysomal fraction of proliferating cells. Furthermore, an inverse relationship between the concentration of G-actin and eNOS expression was observed in endothelial cells subjected to pharmacological alteration of their cytoskeleton; lower G/F-actin ratios correlated with increased eNOS expression. Our findings provide some insight into how endothelial cells may use the dynamic organization of the actin cytoskeleton to regulate expression of an enzyme that is crucial to vascular homeostasis. **(*Circ Res*. 2004;95:488-495.)**

Key Words: endothelial nitric oxide synthase ■ mRNA binding protein ■ mRNA stability ■ 3′ untranslated region ■ cytoskeletal dynamics

Nitric oxide (NO·) is produced in vascular endothelial cells by the endothelial isoform of nitric oxide synthase (eNOS).[1] NO· is crucial to the maintenance of vascular homeostasis through its vasodilator activity,[1] and its ability to inhibit smooth muscle growth,[2] platelet aggregation,[3] and leukocyte adhesion.[4] Although eNOS is constitutively expressed, several biophysical and biochemical stimuli that have been implicated in vascular pathophysiology can modify the expression of eNOS. In cultured cells, shear stress,[5] lysophosphatidylcholine,[6] low concentrations of oxidized low-density lipoprotein,[7] oxidized linoleic acid,[8] 3-hydroxy-3-methylglutaryl coenzyme A reductase inhibitors,[9] and hydrogen peroxide[10] increased eNOS expression. In contrast, exposure of cultured cells to tumor necrosis factor-α,[11] hypoxia,[12] lipopolysaccaride,[13] thrombin,[14] and high concentrations of oxidized low-density lipoprotein[15] all decreased eNOS levels. For many of these stimuli, modulation of eNOS mRNA stability plays an essential role in determining eNOS expression. However, the details of the mechanism(s) responsible for these alterations in eNOS transcript half-life have not been fully elucidated.

One of the most potent stimuli for eNOS expression in vascular endothelial cells is growth. In proliferating bovine aortic endothelial cells (BAECs), eNOS mRNA was increased 4- to 5-fold as compared with cells several days after confluence.[16] This enhanced expression was entirely attributable to an increase in eNOS mRNA stability; eNOS mRNA half-life was 2 to 3 times greater in proliferating BAECs versus confluent cells.[17] Previously, we identified a cis-acting sequence element within the proximal portion of the eNOS 3′ untranslated region (3′UTR) that was associated with regulation of eNOS mRNA stability. A 51-kDa cytoplasmic protein was observed to bind to this sequence, and ribonucleoprotein binding was inversely related to eNOS mRNA stability. Furthermore, deletion of the cis-acting sequence element led to stabilization of chimeric eNOS mRNA, suggesting that the 51-kDa ribonucleoprotein may be a destabilizing factor.

The purpose of the present study was to determine the identity of the 51-kDa ribonucleoprotein and further characterize its role in eNOS expression. The RNA–protein com-

Original received July 11, 2003; resubmission received March 31, 2004; revised resubmission received June 29, 2004; accepted July 2, 2004.
From the Division of Cardiology, Emory University, Atlanta, Ga.
Correspondence to Charles D. Searles, Division of Cardiology, Emory University, 1639 Pierce Dr, WMB 319, Atlanta, GA 30322. E-mail csearle@emory.edu

plex was purified and subjected to mass spectrometric analysis. The results indicated that monomeric actin was the predominant protein in the eNOS 51-kDa ribonucleoprotein complex. Subsequently, the relationship between the actin cytoskeleton and eNOS mRNA was examined microscopically and biochemically. Further studies were performed to examine the role of the G-actin versus filamentous actin (F-actin) concentration in regulating eNOS expression. Our findings provide evidence for a novel mechanism that uses the dynamic properties of the actin cytoskeleton to regulate eNOS expression.

Materials and Methods

Materials

All materials for cell culture were from Cellgro. Biotin-16-uridine-5′-triphosphate and digoxigenin-11-uridine-5′-triphosphate were obtained from Roche. Streptavidin-agarose beads and DNase I were purchased from Sigma. Purified nonmuscle actin was obtained from Cytoskeleton Inc. Thymosin β-4 was purchased from Advanced Chemtech. Alexa Fluor 488 DNase I, Alexa Fluor 568 phalloidin, and jasplakinolide were purchased from Molecular Probes. Swinholide A was purchased from Biomol Research Laboratories. Tri Reagent was obtained from Molecular Research.

Cell Culture

BAECs were cultured in medium (M199) containing 10% fetal calf serum as described.[8] Experiments were conducted on cells between passages 3 and 9.

UV-Crosslinking Assays

Cytosolic protein fractions were prepared according to the protocol by Dignam et al.[18] UV-crosslinking assays were performed essentially as described previously[17] with the exception that biotinylated riboprobes were used. Biotinylated riboprobes of the eNOS 3′UTR (545 nt) were prepared by in vitro transcription reactions using T7 RNA polymerase (Ambion) and biotin-16-uridine-5′-triphosphate. After the UV-crosslinking reaction, the biotinylated RNA–protein complexes were separated on a 12% SDS-polyacrylamide gel, electroblotted to positively charged nylon membranes, and detected using the Bright Star Biodetect Kit (Ambion).

Purification and Identification of eNOS mRNA-Binding Protein

Cytosolic protein was extracted from confluent endothelial cells as described for the UV-crosslinking assay. Protein extracts were concentrated using a centrifugation filter device (10 000 molecular weight cutoff; Millipore), and 5 mg of concentrated cytosolic protein was incubated with 20 μg of biotinylated eNOS 3′UTR riboprobes under UV-crosslinking assay conditions. The biotinylated RNA–protein complex was loaded on 0.3 mL of streptavidin-agarose beads that had been previously washed extensively with buffer containing HEPES (10 mmol/L, pH 7.4). The beads were washed with 50 mL of HEPES buffer containing 0.4 mol/L urea. The beads were subsequently boiled in 0.3 mL of Laemmli buffer for 5 minutes and briefly centrifuged. The supernatant was loaded onto multiple lanes of a 12% SDS-polyacrylamide gel and separated by electrophoresis. The gel was divided into 2 parts; one part was stained with Coomassie blue and the other part was processed for detection of biotinylated protein. The target band was excised from the gel, and the protein was digested with trypsin before being subjected to nanospray MS/MS analysis on a Q-Tof mass spectrometer (Emory University Microchemical Facility and Yale Cancer Center Mass Spectrometry Resource Laboratory). Before analysis, an internal peptide calibrant (Glu-fibrinogen) was added to the digest, and the sample was cleaned with a C-18 packed ZipTip. MS/MS spectra were searched using the Sequest search program, which was performed against the NCBI nr protein database.

Fluorescence Confocal Microscopy

Details of G-actin and F-actin staining are described in the online data supplement available at http://circres.ahajournals.org. Alexa Fluor 488 DNase I was used for staining G-actin in BAECs, and Alexa Fluor 568 phalloidin was used for staining F-actin. Cells were examined using a Zeiss LSM 510 laser scanning confocal microscope.

Fluorescence In Situ Hybridization

ENOS templates were transcribed with T7 RNA polymerase and Sp6 RNA polymerase (Ambion) in the presence of digoxigenin-11-uridine-5′-triphosphate to generate a 693-bp sense riboprobe and a 705-bp antisense probe, respectively. Details of the hybridization process are described in online data supplement.

Cell Fractionation and RNA Quantification

Polysomal fractions were isolated using a sequential detergent/salt extraction procedure described previously.[19–21] Total RNA was isolated from each polysome fractions using Tri Reagent and assessed by the A_{260}/A_{280} absorbance ratio. ENOS mRNA was quantified by real-time polymerase chain reaction (PCR) of cDNA derived from reverse transcribed total RNA; 5 μg of total RNA from each fraction was reverse-transcribed using either an oligo dT-primer (5′-GCGAGCTCCGCGGCCGCGT$_{(12)}$-3′) or random hexamer primer and Superscript III reverse-transcriptase (Invitrogen). Real-time PCR was performed on 2 μL of the reverse transcription reaction, using the Light Cycler (Roche) as described earlier.[22] The bovine eNOS primers, 5′-CCCAACAGCCCCACGCTGACC-3′ and 5′-CACTGT-GATGGCCGAGCG AAGGTTG-3′ were located on different exons. 18S rRNA was also quantified in each sample.

G-actin/F-actin In Vivo Assay

Filamentous actin (F-actin) and free globular-actin (G-actin) content in BAECs were measured using an assay kit obtained from Cytoskeleton Inc. Details of the assay are described in the online data supplement.

Northern Blotting

Northern analysis was performed as previously described.[8]

Results

Purification of the eNOS 3′UTR-Binding Protein and Binding of Monomeric Actin to the eNOS 3′UTR

Our strategy for purifying the eNOS 3′UTR binding protein involved using streptavidin-agarose beads to isolate biotinylated and crosslinked eNOS 3′UTR/protein complexes from endothelial cell extracts. An example of the protein eluted from the streptavidin-agarose beads is shown in Figure 1A. Because our purification scheme involved isolation of a biotinylated RNA–protein complex, the target band was identified based on molecular mass and affirmation that the band was biotinylated. The prominent higher molecular mass band seen in Figure 1A was not biotinylated, and its size was consistent with streptavidin that had become detached from the agarose beads.

Analysis of 5 MS/MS spectra indicated that monomeric actin was the predominant protein present in the target band. Although analysis of the MS/MS spectra was able to rule out the presence of the α actin isoform, the spectra were consistent with peptide fragments common to the β and γ isoforms of actin. These results suggest that monomeric actin (either β or γ) is an integral part of the 51-kDa ribonucleoprotein that

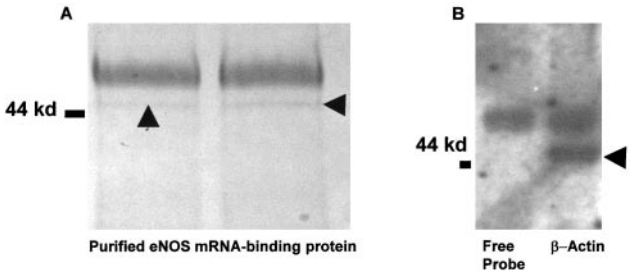

Figure 1. A, eNOS ribonucleoprotein purified from BAEC cytoplasmic extract. 12.5% SDS-polyacrylamide gel of purified protein, stained with Coomassie blue. The arrow heads indicate the target protein in 2 separate experiments; this band was subjected to mass spectrometric analysis. B, UV-crosslinking experiment demonstrating binding of purified monomeric actin to the 3′UTR of eNOS. 2 μg of monomeric actin was incubated with 0.1 μg of biotinylated RNA probe, and UV-crosslinking analysis was performed. "Free probe" lane indicates assay performed in the absence of protein. This blot is representative of three separate experiments.

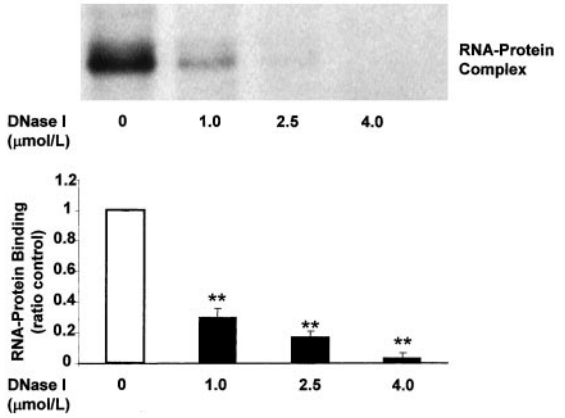

Figure 2. The effect of DNase I on eNOS ribonucleoprotein formation. Top panel shows the RNA-protein UV-crosslinking analysis of cell extracts pre-incubated with increasing concentrations of DNase I (0, 1.0 μmol/L, 2.5 μmol/L, 4.0 μmol/L). Bottom panel shows the densitometric analysis of at least 3 experiments, expressed as the ratio of ribonucleoprotein binding relative to control. *Significant difference compared with control ($P<0.01$, Dunnett test after 1-way ANOVA).

interacts with the eNOS 3′UTR. Because of the intrinsic nature of mass spectrometry, there may be other proteins in the sample that were not detected but were part of the ribonucleoprotein complex. Despite this possibility, the discrepancy in size between actin (43 kDa) and the 51-kDa protein may be attributable in part to the presence of a crosslinked fragment of eNOS 3′UTR (≈43 nt).

To verify that monomeric actin is able to interact with eNOS mRNA, RNA–protein UV-crosslinking analysis was performed with biotinylated eNOS 3′UTR and purified, monomeric nonmuscle actin (80% β-actin, 20% γ-actin; 99% pure; Cytoskeleton Inc.). On SDS-PAGE (Figure 1B), there was a band with a molecular mass similar to the 51-kDa ribonucleoprotein seen in cytoplasmic extracts. There was also a biotinylated band with a higher molecular mass (above the arrowhead-marked band in Figure 1B). This band was observed despite the omission of protein from the assay, suggesting that it was incompletely digested riboprobe. Of note, up to 2 μg of monomeric actin was required to detect a signal under these assay conditions. This may reflect the physiological concentration of monomeric actin needed for interaction with the eNOS 3′UTR, or it may indicate the absence of a factor that facilitates the actin–eNOS interaction in cytoplasmic extracts at lower actin concentrations.

Effect of Actin Monomer Binding Proteins on Protein Binding to the eNOS 3′UTR

We further examined the interaction of actin with the eNOS 3′UTR by determining the effects of 2 actin monomer sequestering proteins on formation of the eNOS 51-kDa ribonucleoprotein. Cytoplasmic extracts were preincubated (30 minutes) with increasing concentrations of DNase I, a protein known to bind specifically G-actin,[23] and UV-crosslinking analysis was performed; 1.0, 2.5, and 4.0 μmol/L DNase I inhibited eNOS ribonucleoprotein formation by 70%, 83%, and 97%, respectively (Figure 2). Similar findings were observed after preincubation (30 minutes) with thymosin β-4, the main actin monomer-sequestering protein in eukaryotic cells[24] (Figure 3); 10 and 50 μmol/L of thymosin β-4 inhibited protein binding by 37% and 70%, respectively. These results indicate that the eNOS mRNA–protein interaction can be competitively inhibited by proteins known to specifically bind and sequester G-actin. This supports the finding that monomeric actin is an integral part of the 51-kDa ribonucleoprotein. Furthermore, these results provide some evidence as to which subdomain of monomeric actin interacts with eNOS mRNA; the actin/eNOS interaction must involve the DNase I and thymosin β-4 binding sites. The binding sites for DNase I and thymosin β-4 are located on oppositely spaced subdomains of actin that bridge an interdomainal cleft, but these subdomains are allosterically coupled.[23,25] Interestingly, another actin monomer-binding protein, profilin, did not inhibit formation of the eNOS ribonucleoprotein complex (data not shown).

G- and F-actin Localization and Quantification in Proliferating Versus Confluent Cells

Because a major property of actin is its ability to exist in 2 forms, G-actin and F-actin, we hypothesized that the interaction between monomeric actin and eNOS mRNA is related to the relative concentration of cytoplasmic G-actin versus F-actin. G-actin and F-actin pools in proliferating and confluent cells were fluorescently stained and examined by laser scanning confocal microscopy (Figure 4). In confluent cells, there was intense, diffuse staining for F-actin, most notably in the cell periphery, at sites of cell–cell contact. There was also staining for actin fibers centrally, which are likely involved in cell–substratum adhesion. Staining for G-actin showed an area of intense perinuclear localization. In contrast to confluent cells, the diffuse network of F-actin was not present in proliferating cells; F-actin appeared to be concentrated near the cell periphery. G-actin staining in these cells was much less intense than in confluent cells, and perinuclear localization was absent.

The effect of cell growth on actin cytoskeleton organization was quantified by measuring the ratio of G-actin to F-actin. In confluent cells, the G/F-actin ratio of 1 is consis-

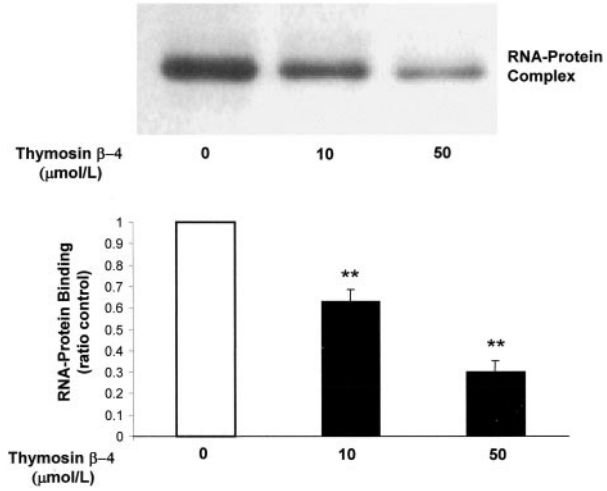

Figure 3. The effect of thymosin β-4 on protein binding to the eNOS 3′UTR. Top panel shows a representative UV-crosslinking analysis of endothelial cell extracts pre-incubated with 10 μmol/L and 50 μmol/L thymosin β-4. Bottom panel shows the densitometric analysis of 3 separate experiments, expressed as the ratio of ribonucleoprotein binding relative to control. *Significant difference in binding activity compared with nonpretreated extracts ($P<0.01$, Dunnett test after 1-way ANOVA).

tent with a high concentration of monomeric actin that is present in nonmuscle cells at basal state.[26] The confluent cell G/F-actin ratio was 2-fold greater than that of proliferating cells (Figure 5), indicating a relatively higher concentration of monomeric actin and a lower concentration of F-actin in confluent cells. The observation of increased G-actin in confluent cells, together with the finding that monomeric actin is a major component of a ribonucleoprotein associated with eNOS mRNA destabilization, suggests that actin cytoskeletal organization is important to the growth-related posttranscriptional regulation of eNOS expression.

Localization of eNOS mRNA and G-actin in Confluent Versus Proliferating BAECs

The localization of eNOS transcripts relative to G-actin was examined by confocal microscopy (Figure 6). Simultaneous fluorescence in situ hybridization of eNOS mRNA and G-actin fluorescent staining were performed on cells in the 2 growth states. In confluent cells, eNOS mRNA was concentrated in the perinuclear region and this localization correlated with the distribution of the most intense G-actin staining. In proliferating cells, eNOS mRNA was found to be more diffuse and not to be colocalized with G-actin. These images demonstrate growth-related differences in the relationship between G-actin and eNOS mRNA in whole cells.

To further characterize growth-related differences in eNOS mRNA localization, an analysis of eNOS mRNA levels in different subcellular polysomal fractions was performed. The free polysome fraction (FP) contains soluble cellular components including G-actin, whereas the cytoskeletal-bound polysome (CBP) fraction contains cellular components associated with cytoskeletal filaments (F-actin) and other cell matrix material. Polysomes associated with cell membranes and the endoplasmic reticulum are found in the membrane-bound polysome (MBP) fraction.

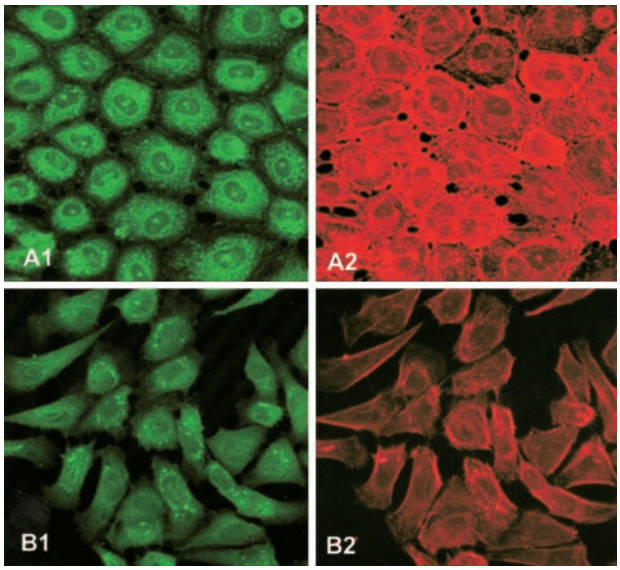

Figure 4. Confocal fluorescent images of actin cytoskeleton in BAECs. A1 and A2, Distribution of G-actin (green) and F-actin (red) in confluent endothelial cells. B1 and B2, Distribution of G-actin (green) and F-actin (red) in proliferating endothelial cells. Cells were stained with Alexa Fluor 488 DNase I (G-actin) and Alexa Fluor 568 phalloidin (F-actin). The images shown are representative of the results observed in 3 experiments.

The eNOS transcripts from proliferating cells were relatively more enriched in the CBP fraction, with a CBP/FBP ratio of 2.7 compared with a ratio of 0.37 for confluent cells (Figure 7). Conversely, eNOS transcripts were enriched in FP fraction of confluent cells. There was no statistical difference in the amount of eNOS mRNA that localized to the MBP fractions, indicating a relatively stable amount of eNOS mRNA in this fraction during cell growth. These results support the concept that localization of eNOS mRNA changes with cell growth; eNOS transcripts in proliferating cells localize to cytoskeletal filaments, and, as cells stop

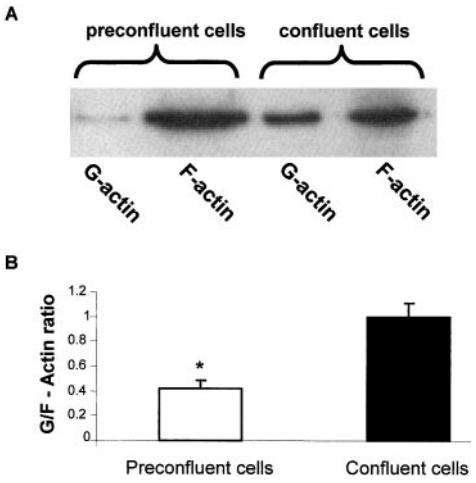

Figure 5. Quantification of G/F-actin ratio in preconfluent and confluent endothelial cells. A, Representative Western blot of G- and F-actin from preconfluent and confluent cells. B, Grouped densitometric data for 3 separate experiments, expressed as the ratio of G-actin-to-F-actin. *Significant difference in G-/F-actin ratio of preconfluent cells versus confluent cells ($P<0.0045$, unpaired t test).

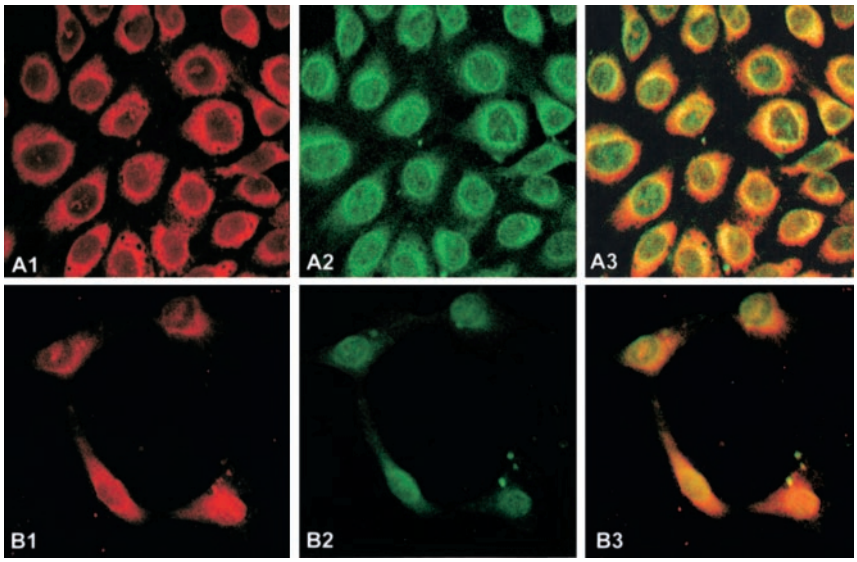

Figure 6. Localization of eNOS mRNA and G-actin in BAECs at different states of cell growth. Confluent endothelial cells (A1, A2, A3) and preconfluent cells (B1, B2, B3) were subjected to fluorescence in situ hybridization with a 705-bp antisense eNOS mRNA probe (red; A1, B1) and G-actin fluorescence staining with Alexa Fluor 488 DNase I (green; A2, B2). A3 and B3 are overlays of A1, B1 and A2, B2, respectively. Areas of yellow staining represent colocalization of eNOS mRNA and G-actin. The images shown are representative of results observed in 3 experiments.

proliferating, the eNOS mRNA shifts to noncell matrix polysomes. Furthermore, because G-actin is largely found in the free polysomal fraction, the enrichment of confluent cell eNOS mRNA in this fraction is consistent with the colocalization of G-actin and eNOS mRNA that was observed in our confocal microscopy studies.

Effect of Actin-Targeted Agents on Protein Binding to the eNOS 3′UTR and eNOS Expression

Two different actin-binding agents were used to assess the effects of specific actin perturbation on eNOS mRNA levels and eNOS ribonucleoprotein formation. Jasplakinolide (JASPA) is a natural marine sponge product that is a potent inducer of actin polymerization and a stabilizer of actin filaments in vitro.[27] Swinholide A (SWA) is a dimeric macrolide that is known to have 2 effects on actin in vitro: it severs actin filaments and it dimerizes actin monomers.[27,28] The G/F-actin ratios were quantified in BAECs after treatment with JASPA or SWA (Figure 8). JASPA, as expected, lowered the G/F-actin ratio, but SWA appeared to increase the G/F-actin ratio. Although initial analysis of the S100 fraction indicated that SWA-treated cells contained an abundance of G-actin, further sedimentation at 150 000*g* for 3 hours revealed that a majority was actually dimeric actin (data not shown). Despite different actions, these 2 drugs had similar effects on the eNOS ribonucleoprotein formation and eNOS mRNA expression in BAECs. UV-crosslinking analysis of cells treated with 0.5 μmol/L JASPA resulted in a 37% decrease in binding of the 51-kDa ribonucleoprotein. A 37% decrease in binding activity was also observed after treatment with 100 nmol/L of SWA (Figure 8). JASPA treatment led to a dose-dependent increase in eNOS mRNA levels, which were increased 2-fold with 0.5 μmol/L JASPA (Figure 8). eNOS mRNA levels were also increased 2-fold after treatment with 100 nmol/L of SWA.

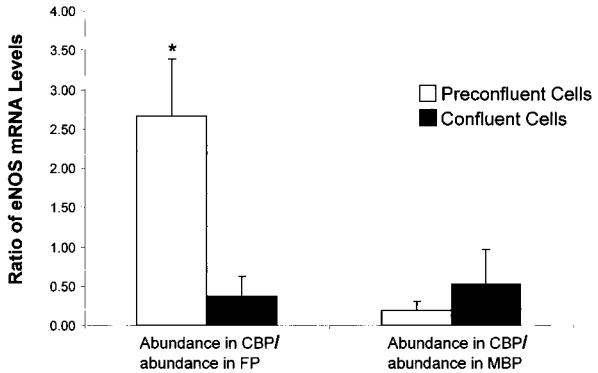

Figure 7. Distribution of eNOS mRNA transcripts between free polysomes (FP), cytoskeletal-bound polysomes (CBP), and membrane-bound polysomes (MBP). The eNOS mRNA levels in different polysome fractions from preconfluent and confluent BAECs were measured by real-time reverse-transcriptase polymerase chain reaction and normalized to the level of 18S rRNA. The distribution of eNOS mRNA is expressed as the ratio of eNOS mRNA in CBP to that in FP, or as the ratio of CBP eNOS mRNA to that in MBP. *Significant difference in the CBP/FP ratio in preconfluent cells versus confluent cells (3 separate experiments; $P=0.0420$, unpaired t test). $P=0.5252$ for comparison of CBP/MBP in preconfluent cells versus confluent cells (3 separate experiments; unpaired t test).

These studies show that pharmacological lowering of the proportion of G-actin in confluent cells leads to decreased binding of the 51-kDa ribonucleoprotein to eNOS mRNA and an increase in eNOS expression. This was achieved by drugs with different mechanisms of action. Furthermore, JASPA increased eNOS mRNA stability (online Figure I). These results are consistent with a posttranscriptional regulatory mechanism whereby the cytosolic interaction of eNOS mRNA with monomeric actin leads to its destabilization and decreased expression.

Discussion

Previously, we characterized a cis-acting sequence element in the eNOS 3′UTR that was involved in growth-related changes in eNOS mRNA stability.[17] In the current studies, we identified monomeric actin as the predominant component of a 51-kDa cytoplasmic ribonucleoprotein that binds to the eNOS 3′UTR. Our results indicate that actin binding to the eNOS 3′UTR in cells at different growth states is related to

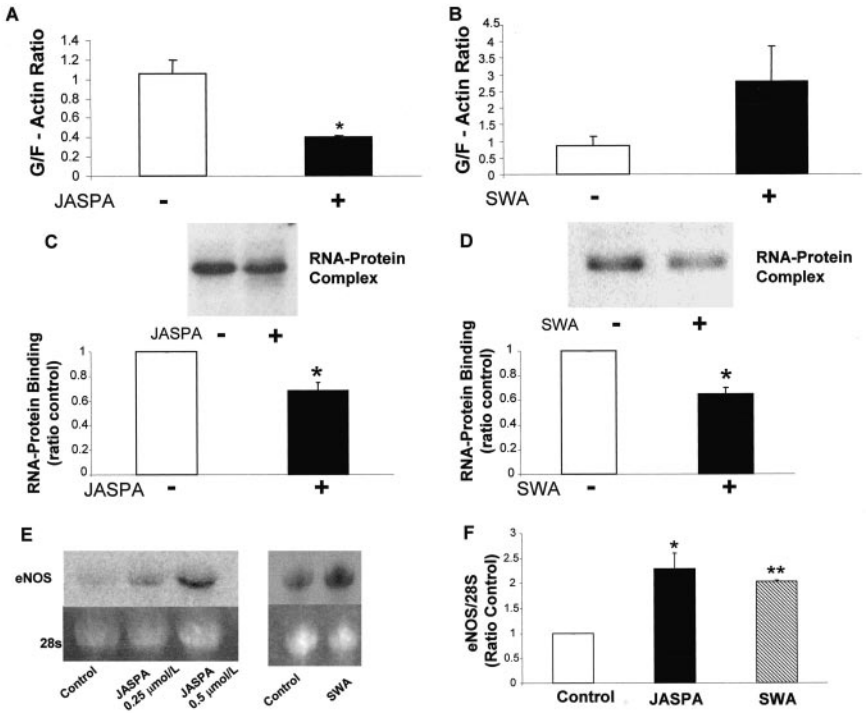

Figure 8. The effect of jasplakinolide (JASPA) and swinholide A (SWA) on G/F-actin ratio, eNOS ribonucleoprotein formation, and eNOS expression. A, G/F actin ratio in confluent BAECs treated with 0.5 μmol/L JASPA for 10-hour cells versus untreated cells (3 separate experiments, *P=0.0446 versus control; 2-tailed unpaired t test). B, Ratio of G/F-actin in cells treated with 100 nmol/L swinholide A for 8 hours versus untreated cells (3 separate experiments, P=0.3057 versus control; 2-tailed, unpaired t test). The presence of dimeric actin in the SWA-treated S100 fraction was confirmed by further sedimentation of this fraction. C, UV-crosslinking analysis of confluent cells treated with JASPA 0.5 μmol/L for 10 hours. Top panel shows a representative blot of UV-crosslinking assay. Lower panel shows the grouped densitometric data (4 separate experiments, mean±SEM), expressed as ratio of RNA-to-protein binding relative to control binding (*P=0.0180 versus control; paired 2-tailed t test). D, UV-crosslinking analysis of confluent cells treated with SWA 100 nmol/L for 8 hours. Top panel shows representative blot and bottom panel shows the grouped densitometric data (3 separate experiments, mean±SEM), expressed as ratio of RNA-to-protein binding relative to control (*P=0.0217 paired 2-tailed t test). E, Representative Northern blots of cells treated with JASPA 0.25 μmol/L or 0.5 μmol/L for 10 hours and cells treated with 100 nmol/L SWA for 8 hours. F, Grouped densitometric data (mean±SEM) for 3 separate experiments using 0.5 μmol JASPA or 100 nmol/L swinholide A. * P<0.01 versus control, **P<0.05 versus control.

endothelial cytoskeleton organization, specifically the relative concentration of G-actin versus F-actin. Furthermore, pharmacological perturbation of the G/F-actin ratio led to changes in eNOS expression that were consistent with monomeric actin being part of destabilization mechanism for eNOS mRNA.

The actin cytoskeleton has been shown to be intimately involved in the maintenance of endothelial integrity by providing the structural framework for cell shape, cell movement, and cell–cell and cell–substratum interactions.[29] Within the cells of a confluent monolayer, actin microfilaments are distributed peripherally, known as the dense peripheral band, and centrally, known as central microfilaments (or stress fibers).[30] These bundles of microfilaments undergo dynamic changes in response to physiological and pathological stresses, including shear stress, vascular pressure, and wound healing processes.[29,31,32] Less is known about the importance of G-actin in cytoskeletal function. Our data show dynamic changes in cytoskeleton organization during cell growth and indicate a role for G-actin concentration in regulating endothelial gene expression.

There is increasing evidence that mechanisms involved in cytoplasmic mRNA metabolism are under the dynamic control of various cytoskeletal elements. It has been shown that for some proteins, the subcellular localization and targeting of their mRNAs plays a significant role in determining efficient translation and proper protein localization.[33] This has led to the concept that transport and localization of mRNA involves cytoskeletal components.[33] Because mRNA stability is often closely linked to translation, cytoskeleton-mediated transport and localization of mRNA to appropriate polysomal fractions may regulate its turnover. Our results indicate that localization of eNOS mRNA varies with cell growth and that this is likely related to changes in the actin cytoskeleton.

A relationship between mRNA stability and the state of actin cytoskeletal polymerization has been described for certain highly unstable lymphokine mRNAs.[34,35] Cytochalasin-induced disruption of lymphocyte microfilaments resulted in more stable IL-2 and tumor necrosis factor-α mRNAs, and this was associated with an altered subcellular localization of destabilizing RNA-binding proteins. These proteins could be immunoprecipitated with anti-actin antibodies. In addition, the stability and expression of actin mRNA itself are inversely related to the cytoplasmic level of G-actin, but not F-actin.[36] This negative autoregulatory mechanism involves the actin mRNA 3′UTR; actin mRNA lacking the 3′UTR is not subject to autoregulatory inhibition.

An association between actin cytoskeleton organization and eNOS expression has been described previously. HMG-CoA reductase inhibitors posttranslationally inhibit Rho activity and upregulate eNOS expression posttranscriptionally.[9] Endothelial cells that overexpressed a dominant-negative Rho A mutant exhibited decreased actin stress fiber formation and increased eNOS expression.[37] Mice treated with a Rho inhibitor or the actin cytoskeleton disrupter cytochalasin D showed increased vascular eNOS expression and activity, and these changes were associated with a decrease in cerebral infarction size after middle cerebral artery occlusion.[37]

The endothelial actin cytoskeleton is regulated by many stimuli that have also been shown to influence eNOS expres-

sion, but whether the mechanism for growth-related regulation is applicable to other conditions is uncertain. We have performed UV-crosslinking analysis on cytoplasmic extracts from cells exposed to shear stress, hydrogen peroxide, and mevastatin to determine whether these stimuli have an effect on actin binding to the eNOS 3′UTR. All of these stimuli have been shown to modulate endothelial actin cytoskeleton organization[31,32,37,38] and upregulate eNOS expression.[5,10,39] Shear stress did not significantly affect actin binding to the eNOS 3′UTR, but treatment with H_2O_2 resulted in a dramatic decrease in binding activity (online Figure II). Mevastatin also decreased binding activity, but this was not significant statistically. Based on these results, a common link between cell growth and other stimuli in their mechanism(s) for regulating eNOS expression may be endothelial cell response to oxidative stress.

In this study, we show that purified, monomeric actin bound to the eNOS 3′UTR but did so when microgram quantities of protein were used in the UV-crosslinking reaction. Although at first glance the quantity of actin used in this experiment seems excessive for it to reflect a physiological role in vivo, it must be noted that actin is the most abundant protein in most eukaryotic cells, comprising 1% to 5% of total cellular protein in nonmuscle cells, and its intracellular concentration approximates that used in the present in vitro experiments. Alternatively, binding of actin to eNOS transcripts at lower concentrations of actin may be facilitated by other factors. The intracellular concentration of monomeric actin in cells at basal state far exceeds the critical concentration for actin polymerization determined under physiological salt conditions in vitro.[26] This high intracellular concentration of G-actin is able to be achieved because of cytoplasmic proteins that can bind and sequester the monomers, effectively raising the critical concentration for polymerization. We were unable to identify any other proteins in our purified ribonucleoprotein sample, but we cannot exclude that the interaction between actin and eNOS mRNA may be facilitated by an actin-binding protein. A recent study identified a direct interaction between actin and eNOS protein in pulmonary artery endothelial cells.[40] This study used concentrations of G-actin that approximate the concentrations used in our UV-crosslinking assays, suggesting that this amount of monomeric actin may be physiologically relevant for eNOS regulation in vivo.

In this study, we provide some insight into how the endothelial cell may use the major property of actin (its ability to exist as a monomer or polymer) to regulate eNOS mRNA stability. The molecular details of how the actin/eNOS mRNA interaction regulates eNOS mRNA stability and expression remains to be determined, but it may involve cytoskeletal-mediated mRNA transport, localization, and subsequent translation. Included in this mechanism may be the recruitment of specific degradative enzymes to a G-actin associated ribonucleoprotein complex. Although human eNOS mRNA is also subject to posttranscriptional regulation and demonstrates multiple protein/3′UTR interactions,[41] the relevance of the mechanism described in the current studies to human eNOS expression is unknown. Future studies of the actin/eNOS mRNA interaction will need to examine its role in eNOS mRNA localization and metabolism. These studies should provide further mechanistic insight into the regulation of eNOS expression and the relationship between vascular gene expression and cytoskeletal organization.

Acknowledgments

This study was supported by National Institutes of Health (NIH) grant HL04062-01.

References

1. Palmer RM, Ferrige AG, Moncada S. Nitric oxide release accounts for the biological activity of endothelium-derived relaxing factor. *Nature*. 1987; 327:524–526.
2. Garg UC, Hassid A. Nitric oxide-generating vasodilators and 8-bromocyclic guanosine monophosphate inhibit mitogenesis and proliferation of cultured rat vascular smooth muscle cells. *J Clin Invest*. 1989;83: 1774–1777.
3. Alheid U, Frolich JC, Forstermann U. Endothelium-derived relaxing factor from cultured human endothelial cells inhibits aggregation of human platelets. *Thromb Res*. 1987;47:561–571.
4. Kubes P, Suzuki M, Granger DN. Nitric oxide: an endogenous modulator of leukocyte adhesion. *Proc Natl Acad Sci U S A*. 1991;88:4651–4655.
5. Nishida K, Harrison DG, Navas JP, Fisher AA, Dockery SP, Uematsu M, Nerem RM, Alexander RW, Murphy TJ. Molecular cloning and characterization of the constitutive bovine aortic endothelial cell nitric oxide synthase. *J Clin Invest*. 1992;90:2092–2096.
6. Zembowicz A, Tang JL, Wu KK. Transcriptional induction of endothelial nitric oxide synthase type III by lysophosphatidylcholine. *J Biol Chem*. 1995;270:17006–17010.
7. Hirata K, Miki N, Kuroda Y, Sakoda T, Kawashima S, Yokoyama M. Low concentration of oxidized low-density lipoprotein and lysophosphatidylcholine upregulate constitutive nitric oxide synthase mRNA expression in bovine aortic endothelial cells. *Circ Res*. 1995;76:958–962.
8. Ramasamy S, Parthasarathy S, Harrison DG. Regulation of endothelial nitric oxide synthase gene expression by oxidized linoleic acid. *J Lipid Res*. 1998;39:268–276.
9. Laufs U, La Fata V, Plutzky J, Liao JK. Upregulation of endothelial nitric oxide synthase by HMG CoA reductase inhibitors. *Circulation*. 1998;97: 1129–1135.
10. Drummond GR, Cai H, Davis ME, Ramasamy S, Harrison DG. Transcriptional and posttranscriptional regulation of endothelial nitric oxide synthase expression by hydrogen peroxide. *Circ Res*. 2000;86:347–354.
11. Yoshizumi M, Perrella MA, Burnett JC, Jr., Lee ME. Tumor necrosis factor downregulates an endothelial nitric oxide synthase mRNA by shortening its half-life. *Circ Res*. 1993;73:205–209.
12. McQuillan LP, Leung GK, Marsden PA, Kostyk SK, Kourembanas S. Hypoxia inhibits expression of eNOS via transcriptional and posttranscriptional mechanisms. *Am J Physiol*. 1994;267:H1921–H1927.
13. Lu JL, Schmiege LM, 3rd, Kuo L, Liao JC. Downregulation of endothelial constitutive nitric oxide synthase expression by lipopolysaccharide. *Biochem Biophys Res Commun*. 1996;225:1–5.
14. Eto M, Barandier C, Rathgeb L, Kozai T, Joch H, Yang Z, Luscher TF. Thrombin suppresses endothelial nitric oxide synthase and upregulates endothelin-converting enzyme-1 expression by distinct pathways: role of Rho/ROCK and mitogen-activated protein kinase. *Circ Res*. 2001;89: 583–590.
15. Liao JK, Shin WS, Lee WY, Clark SL. Oxidized low-density lipoprotein decreases the expression of endothelial nitric oxide synthase. *J Biol Chem*. 1995;270:319–324.
16. Arnal JF, Yamin J, Dockery S, Harrison DG. Regulation of endothelial nitric oxide synthase mRNA, protein, and activity during cell growth. *Am J Physiol*. 1994;267:C1381–C1388.
17. Searles CD, Miwa Y, Harrison DG, Ramasamy S. Posttranscriptional regulation of endothelial nitric oxide synthase during cell growth. *Circ Res*. 1999;85:588–595.
18. Dignam JD, Lebovitz RM, Roeder RG. Accurate transcription initiation by RNA polymerase II in a soluble extract from isolated mammalian nuclei. *Nucleic Acids Res*. 1983;11:1475–1489.
19. Campbell GP, Hesketh JE. Distribution of glutathione peroxidase mRNAs between free and cytoskeletal-bound polysomes in H4 hepatoma cells. *Biochem Soc Trans.* 1996;24:189S.

20. Hesketh JE, Campbell GP, Whitelaw PF. c-myc mRNA in cytoskeletal-bound polysomes in fibroblasts. *Biochem J*. 1991;274: 607–609.
21. Hovland R, Campbell G, Pryme I, Hesketh J. The mRNAs for cyclin A, c-myc and ribosomal proteins L4 and S6 are associated with cytoskeletal-bound polysomes in HepG2 cells. *Biochem J*. 1995;310: 193–196.
22. Szocs K, Lassegue B, Sorescu D, Hilenski LL, Valppu L, Couse TL, Wilcox JN, Quinn MT, Lambeth JD, Griendling KK. Upregulation of Nox-based NAD(P)H oxidases in restenosis after carotid injury. *Arterioscler Thromb Vasc Biol*. 2002;22:21–27.
23. dos Remedios CG, Chhabra D, Kekic M, Dedova IV, Tsubakihara M, Berry DA, Nosworthy NJ. Actin binding proteins: regulation of cytoskeletal microfilaments. *Physiol Rev*. 2003;83:433–473.
24. Huff T, Muller CS, Otto AM, Netzker R, Hannappel E. beta-Thymosins, small acidic peptides with multiple functions. *Int J Biochem Cell Biol*. 2001;33:205–220.
25. Ballweber E, Hannappel E, Huff T, Mannherz HG. Mapping the binding site of thymosin beta4 on actin by competition with G-actin binding proteins indicates negative cooperativity between binding sites located on opposite subdomains of actin. *Biochem J*. 1997;327:787–793.
26. Carlier MF, Valentin-Ranc C, Combeau C, Fievez S, Pantoloni D. Actin polymerization: regulation by divalent metal ion and nucleotide binding, ATP hydrolysis and binding of myosin. *Adv Exp Med Biol*. 1994;358: 71–81.
27. Spector I, Braet F, Shochet NR, Bubb MR. New anti-actin drugs in the study of the organization and function of the actin cytoskeleton. *Microsc Res Tech*. 1999;47:18–37.
28. Bubb MR, Spector I, Bershadsky AD, Korn ED. Swinholide A is a microfilament disrupting marine toxin that stabilizes actin dimers and severs actin filaments. *J Biol Chem*. 1995;270:3463–3466.
29. Gotlieb AI, Lee TY. Endothelial repair in atherogenesis. *Curr Top Pathol*. 1999;93:157–166.
30. Lee TY, Rosenthal A, Gotlieb AI. Transition of aortic endothelial cells from resting to migrating cells is associated with three sequential patterns of microfilament organization. *J Vasc Res*. 1996;33:13–24.
31. Kim DW, Langille BL, Wong MK, Gotlieb AI. Patterns of endothelial microfilament distribution in the rabbit aorta in situ. *Circ Res*. 1989;64: 21–31.
32. Langille BL, Graham JJ, Kim D, Gotlieb AI. Dynamics of shear-induced redistribution of F-actin in endothelial cells in vivo. *Arterioscler Thromb*. 1991;11:1814–1820.
33. Hesketh JE. Sorting of messenger RNAs in the cytoplasm: mRNA localization and the cytoskeleton. *Exp Cell Res*. 1996;225:219–236.
34. Henics T, Nagy E, Szekeres-Bartho J. Interaction of AU-rich sequence binding proteins with actin: possible involvement of the actin cytoskeleton in lymphokine mRNA turnover. *J Cell Physiol*. 1997;173: 19–27.
35. Henics T. Microfilament-dependent modulation of cytoplasmic protein binding to TNFalpha mRNA AU-rich instability element in human lymphoid cells. *Cell Biol Int*. 1999;23:561–570.
36. Lyubimova A, Bershadsky AD, Ben-Ze'ev A. Autoregulation of actin synthesis responds to monomeric actin levels. *J Cell Biochem*. 1997;65: 469–478.
37. Laufs U, Endres M, Stagliano N, Amin-Hanjani S, Chui DS, Yang SX, Simoncini T, Yamada M, Rabkin E, Allen PG, Huang PL, Bohm M, Schoen FJ, Moskowitz MA, Liao JK. Neuroprotection mediated by changes in the endothelial actin cytoskeleton. *J Clin Invest*. 2000;106: 15–24.
38. Zhao Y, Davis HW. Hydrogen peroxide-induced cytoskeletal rearrangement in cultured pulmonary endothelial cells. *J Cell Physiol*. 1998; 174:370–379.
39. Laufs U, Liao JK. Post-transcriptional regulation of endothelial nitric oxide synthase mRNA stability by Rho GTPase. *J Biol Chem*. 1998;273: 24266–24271.
40. Su Y, Edwards-Bennett S, Bubb MR, Block ER. Regulation of endothelial nitric oxide synthase by the actin cytoskeleton. *Am J Physiol Cell Physiol*. 2003;284:C1542–C1549.
41. Lai PF, Mohamed F, Monge JC, Stewart DJ. Downregulation of eNOS mRNA expression by TNFalpha: identification and functional characterization of RNA-protein interactions in the 3′UTR. *Cardiovasc Res*. 2003; 59:160–168.

Expanded Materials and Methods

Fluorescence Confocal Microscopy

BAECs were plated onto 22-mm diameter round glass coverslips in six-well clusters. Confluent and preconfluent cells were rinsed quickly in PBS, fixed in freshly prepared 3.7% formaldehyde in PBS for 10 min at room temperature, permeabilized in 0.1% Triton X-100 in PBS for 5 min, and rehydrated in PBS for 10 min. The coverslips were incubated with Alexa Fluor 488 DNase I for 20 min to stain for G-actin and then washed with PBS. Subsequently, the coverslips were incubated with Alexa Fluor 568 phalloidin for 15 min to stain for F-actin and then washed with PBS. Cells on coverslips were mounted onto glass slides in Vectashield.

Fluorescence In Situ Hybridization

BAECs were grown on Falcon CultureSlides and fixed in 4% paraformaldehyde for 10 min. Cells were then immersed in buffer containing Tris (pH 8.0) 10 mmol/L, NaCl 500 mmol/L, and 1 μg/ml proteinase K for 10 min at room temperature, and washed with 0.5 X SSC for 10 min. Cells were prepared for riboprobe hybridization by placing in hybridization buffer containing Tris (pH 8.0) 20 mmol/L, NaCl 0.3 M, EDTA 5 mmol/L, DTT 10 mmol/L, 1x Denhardt's solution, 10% dextran sulfate, 50% formamide, for 3 hours at 42^{O} C. Each slide was incubated with 200 ng of riboprobe (sense or antisense) and 200 μg yeast tRNA, and hybridized overnight at 55^{O} C. The following day, slides were washed twice with 2X SSC and incubated with 20 μg/ml RNase A for 30 min at 37^{O} C. Slides were then washed with 0.1X SSC for 2 hours at 55^{O} C, followed by two 10 min washes with 0.5X SSC at room temperature. Immunohistochemistry was performed on cells using a mouse-anti-digoxigenin primary antibody and a

biotinylated horse-anti-mouse-alkaline phosphatase secondary antibody. Vector Red (Vector Laboratories) was used as the substrate for alkaline phosphatase. Cells were subsequently stained for G-actin and examined with a Zeiss LSM 510 laser scanning confocal microscope, as described above.

G-actin/F-actin In Vivo Assay

Cells were lysed in buffer containing PIPES (pH 6.9) 50 mM, NaCl 50 mM, $MgCl_2$ 5 mM, EGTA 5 mM, glycerol 5%, 0.1% Nonidet P40, 0.1% Triton X-100, 0.1% Tween 20, ATP 1 mM, and a protease cocktail (pepstatin, leupeptin, benzamidine, TAME). Lysed cells were centrifuged at 100,000 X g for 60 minutes at 37^{o}C. Supernatants were saved for analysis of G-actin, and F-actin was obtained from the cell pellet that was resuspended in ice cold dH_2O plus 1 μM cytochalasin-D over 1 hour on ice. G-actin and F-actin levels were determined in equivalent protein aliquots from these fractions by Western analysis using the anti-actin antibody provided in the kit. The ratio of G-actin to F-actin was quantified by scanning densitometry.

Online figure legends:

Figure 1: 5,6-dichloro-1-β-D-ribofuranosylbenzimidazole (DRB)-chase experiment to examine the effect of jasplakinolide (JASPA) on eNOS mRNA stability. Confluent BAECs were treated with 0.5 μmol/L JASPA for 10 hours and then exposed to DRB (60 μmol/L). Total RNA was extracted with Tri Reagent (Molecular Research, Inc.) at 0 hours and 12 hours after addition of DRB. The eNOS mRNA from the two time points was measured by ribonuclease protection assay (RPA), using an in vitro transcribed (Mega Script, Ambion), biotinylated 600 bp antisense riboprobe.

The RPA was performed using reagents, buffers, and protocol provided in the RPA III kit from Ambion. Basically, 10 μg total RNA was hybridized with 374 pg of biotinylated eNOS riboprobe overnight at 42 °C. Single stranded RNA was digested with RNases A and T1, and this reaction was stopped by RNA precipitation. The samples were run on a 9% polyacrylamide gel containing urea. RNA was electroblotted onto a positively charged nylon membrane and detected using the Ambion Bright Star System.

The top panels shows a representative blot of the RPA. Lower panel shows the grouped densitometric data for 3 separate experiments (mean $\pm$ SEM), expressed as percent of the 0 hr time point. Values for the 12 hr time point were 46.2 % $\pm$ 9.4 and 14% $\pm$ 1.2 for JASPA and control respectively. Asterisk indicates a significant difference in eNOS mRNA compared to control ($p = 0.0064$, unpaired t-test).

Figure 2: The effect of hydrogen peroxide (H_2O_2), mevastatin, and laminar shear stress on eNOS ribonucleoprotein formation**.** Top panel shows a representative RNA-protein UV crosslinking analysis of cytoplasmic extracts from cells exposed to either 100 μmol/L H_2O_2 (Sigma) for 24 hours, 10 μmol/L mevastatin (Sigma) for 24 hours, or laminar shear stress (15 dynes/cm^2, cone and plate viscometer with 1^0 angle) for 6 hours. Mevastatin was chemically activated by alkaline hydrolysis prior to its use. Bottom panel shows the densitometric analysis of at least three experiments, expressed as the ratio of ribonucleoprotein binding

relative to control. Asterisk indicates a significant difference in H_2O_2 –treated cells compared to control ($p = 0.0011$; paired, two tailed t-test). For mevastatin-treated cells versus control, $p = 0.3139$ (paired, two tailed t-test). For cells exposed to shear stress versus static control, $p = 0.2243$ (paired, two tailed t-test).

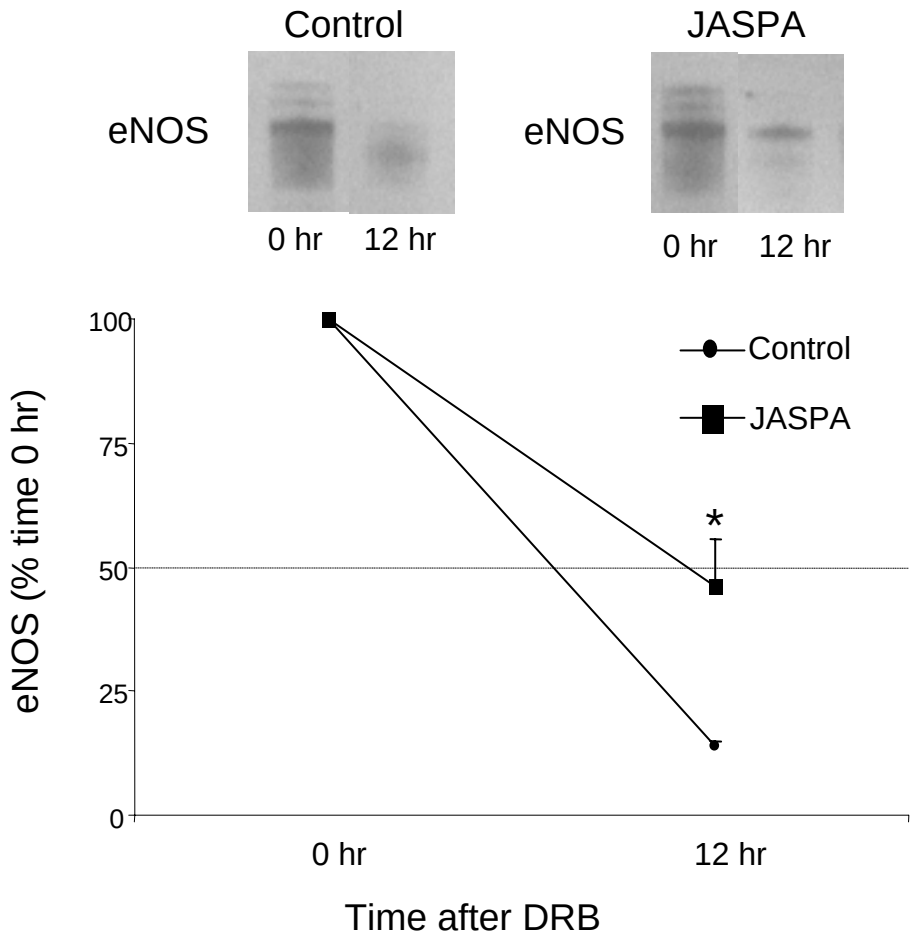

Online Figure 1

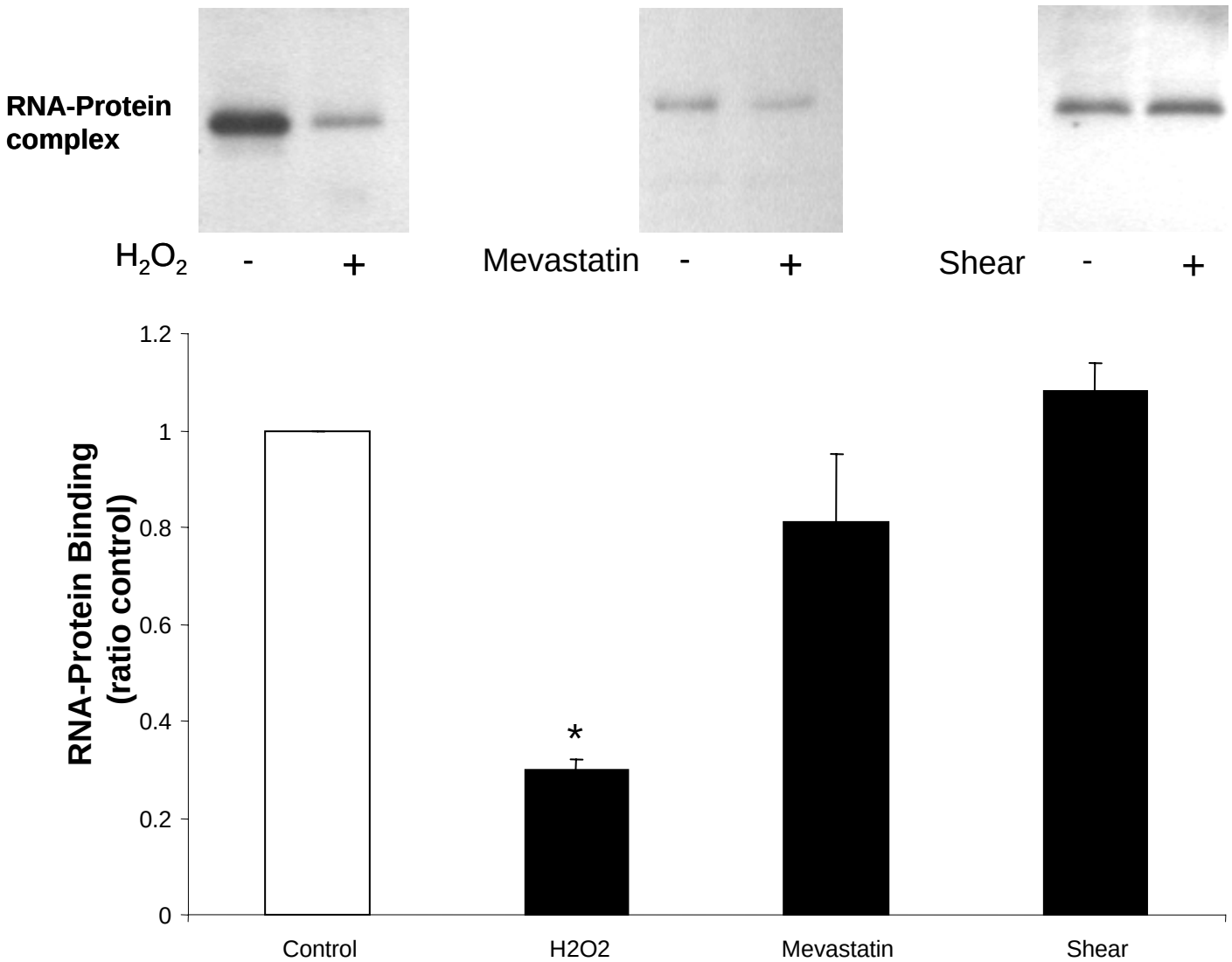

Online Figure 2

Circulation Research
JOURNAL OF THE AMERICAN HEART ASSOCIATION

Actin Cytoskeleton Organization and Posttranscriptional Regulation of Endothelial Nitric Oxide Synthase During Cell Growth

Charles D. Searles, Lucienne Ide, Michael E. Davis, Hua Cai and Martina Weber

Circ Res. 2004;95:488-495; originally published online July 15, 2004;
doi: 10.1161/01.RES.0000138953.21377.80
Circulation Research is published by the American Heart Association, 7272 Greenville Avenue, Dallas, TX 75231

Print ISSN: 0009-7330. Online ISSN: 1524-4571